

Theory of Constrained Cutting: Chip Formation with a Developed Plastic-Deformation Zone

S. I. Petrushin^a and A. V. Proskokov^b

^aTomsk Polytechnic University

^bYurginsk Technological Institute, a Branch of Tomsk Polytechnic University

Abstract—On the basis of slip-line fields, a system for chip formation with a developed plastic-deformation zone is proposed. Equations are derived for the plastic-zone boundaries.

DOI: 10.3103/S1068798X10010119

A model of chip formation with a single conditional shear surface was proposed in [1]. This model cannot be employed in determining the stresses and strains in the blank and chip nor in determining the contact stresses at the working sections of the front and rear cutter surfaces. At the same time, it has been established experimentally that the cut layer is converted to chip in a plastic zone of complex form. Numerous attempts have been made to simulate this zone by constructing slip-line fields. According to plasticity theory, slip lines constitute two families of mutually orthogonal curvilinear coordinates, along which the maximum tangential stress acts. If the kinematically possible slip-line field is constructed, it is possible to calculate the stress–strain state in the chip-formation zone.

In the present work, we adopt two fundamental principles associated with constrained cutting. The first is replacement of the three-dimensional stress–strain state of the cutting zone by planes in the cross sections parallel to the direction of chip departure. This assumption permits solution of the plane plasticity problem, with the construction of slip fields in each cross section. The three-dimensional deformation structure is taken into account by the variation in cut-layer thickness and contact length at the front and rear surfaces of the tool blade. This permits the description of constrained cutting on the basis of formulas established for free cutting.

The second principle is associated with the initial data for calculation of the cutting mechanics. The traditional approach is based on specifying constant tangential stress in the shear plane. In contrast, when we plot a network of slip lines in the plastic region, the initial data are the distributions of the contact stresses at the working areas of the cutters and their values, which correspond to the internal stresses in the plastic zone. In this approach, the change in plastic-zone geometry is attributed to contact processes at the frictional areas of the tool.

The first serious attempt to construct a slip-line field in the chip-formation zone during free orthogonal cutting was made in [2]. Regrettably, although this approach correctly reflects the plastic-deformation pattern on microphotographs of the chip roots, it is unsuitable for calculations, on account of the somewhat arbitrary construction of the slip lines. The stress in the plastic zone may be calculated by the approaches in [3–5]. In that case, however, preference is assigned either to the primary deformation regions adjacent to the free surface of the cut layer and the chip or to the secondary deformation regions around the cutter. Therefore, the development of slip fields in the plastic zone that correspond to experimental data and are also consistent with convenient calculation methods remains a goal that has yet to be attained.

The shape and size of the plasticity zone adjacent to the cutter depends on the frictional conditions of the working surfaces, which are determined by the contact-stress distribution at the front surface and in the chip and also at the rear surface and in the blank.

We now consider the cross section of the chip root in its direction of departure and determine the geometry of the plastic zone adjacent to the front cutter surface where the dynamic front angle $\gamma_d = 0$ (Fig. 1). It is found experimentally that the total contact length l_f of the chip with the front surface consists of plastic (l_{pl}) and elastic (l_{el}) sections of approximately equal extent [6]. Correspondingly, at section l_{pl} , there is friction between the plastically deformable blank and the front cutter surface; at section l_{el} , there is external slipping friction between the chip and the tool. Therefore, for a rigid–plastic model of the blank, the slip-line field will lie above the section l_{pl} and will be absent in the chip in the section l_{el} .

We may approximate the distribution of the normal contact stress at the front surface by the tangential law on the basis of the data in [6]. We also assume that the tangential stress is constant in the plastic section and

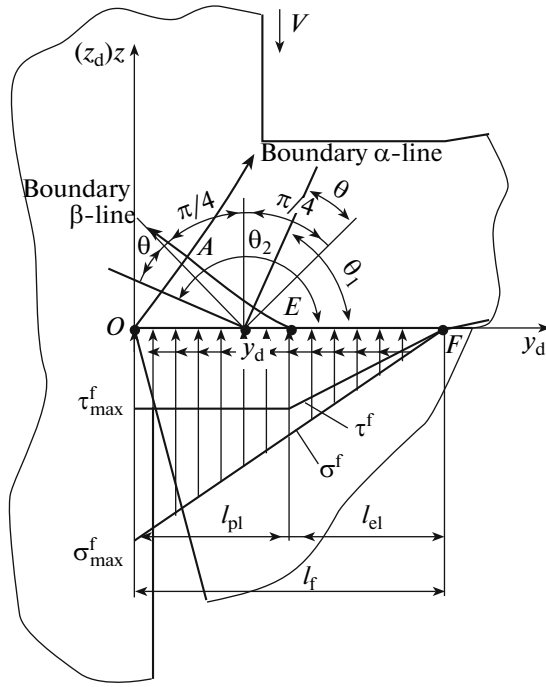


Fig. 1. Application of contact stress to the front cutter surface and slip-line pattern.

declines linearly to zero at the end of contact in the elastic section

$$\sigma^f = \sigma_{\max}^f \left(\frac{y_d}{l_f} \right); \tag{1}$$

$$\tau^f = \begin{cases} \tau_{\max}^f, & 0 \leq y_d \leq l_{pl}; \\ \frac{\tau_{\max}^f}{l_f - l_{pl}} (l_f - y_d), & l_{pl} \leq y_d \leq l_f, \end{cases} \tag{2}$$

where σ_{\max}^f and τ_{\max}^f are the maximum normal and tangential contact stresses at the front surface.

According to the Coulomb–Amonton frictional law, the frictional coefficient at the given point of the contact surface is determined by the ratio of the tangential contact surface to the normal stress at the same point

$$\mu_f = \tau^f / \sigma^f. \tag{3}$$

Substituting the contact stresses at the plastic-contact section from Eqs. (1) and (2) into Eq. (3), we find that

$$\mu_f = \frac{\tau_{\max}^f l_f}{\sigma_{\max}^f (l_f - y_d)} = \mu_{f0} \frac{l_f}{l_f - y_d}, \tag{4}$$

where μ_{f0} is the frictional coefficient at the cutter tip.

It follows from Eq. (4) that, with the given variation in contact stress, the frictional coefficient at the plastic section is not constant but increases from the cutter tip to $y_d = l_{pl}$. In the elastic-contact region, the frictional coefficient, which is the external-friction coefficient

between the elastic chip and the front cutter surface, is constant over the whole elastic contact

$$\mu_f = \mu_{f0} \frac{l_f}{l_f - l_{pl}}.$$

From the plasticity condition, the maximum tangential stress in the plane deformed state may be no larger than $0.5\sigma_y$ [7]. Therefore, $\mu_f < 0.5$ in the plastic-contact region. Hence, the frictional coefficients in the machine pairs cannot be used to estimate chip–cutter contact.

The frictional angle θ at the front surface, which specifies the direction of the primary-stress axes at the contact point y_d , is determined from the frictional coefficient: $\theta = \arctan \mu_f$. The direction of slip-line approach at the contact surface is aligned with the shear lines inclined at $\pi/4$ to the primary normal stress. Hence, the angles at which the slip lines approach the plastic-contact zone are as follows:

for α lines

$$\theta_1 = \frac{\pi}{4} + \theta = \frac{\pi}{4} + \arctan \mu_f;$$

for β lines

$$\theta_2 = \frac{3\pi}{4} + \theta = \frac{3\pi}{4} + \arctan \mu_f.$$

The tangents of θ_1 and θ_2 correspond to the differential equations of the α and β slip lines [7]. In the dynamic coordinate system

$$\alpha - \frac{dz_d}{dy_d} = \tan \left(\frac{\pi}{4} + \arctan \mu_f \right) = \frac{1 + \mu_f}{1 - \mu_f}; \tag{5}$$

$$\begin{aligned} \beta - \frac{dz_d}{dy_d} &= \tan \left(\frac{3\pi}{4} + \arctan \mu_f \right) \\ &= -\cot \left(\frac{\pi}{4} + \arctan \mu_f \right) = -\frac{1 - \mu_f}{1 + \mu_f}. \end{aligned} \tag{6}$$

If we integrate Eqs. (5) and (6), taking account of Eq. (4), we obtain the slip-line equations:

for α lines

$$z_d = y_d - 2\mu_{f0} l_f \ln |l_f(1 - \mu_{f0}) - y_d| + C_I; \tag{7}$$

for β lines

$$z_d = -y_d - 2\mu_{f0} l_f \ln |l_f(1 - \mu_{f0}) - y_d| + C_{II}, \tag{8}$$

where the constants of integration C_I and C_{II} are determined by the coordinates of the plastic contact point.

To construct the complete slip-line field in the chip-formation zone, it is important to have boundary slip lines, where the material passes from the elastic to the plastic state and back. The boundary β lines leave the point $y_d = l_{pl}$, where $z_d = 0$ (point E). Determining C_{II} in Eq. (8), we find that

$$z_d = l_{pl} - y_d + 2\mu_{f0} l_f \ln \left| \frac{l_{el} + \mu_{f0} l_f}{(1 + \mu_{f0}) l_f - y_d} \right|. \tag{9}$$

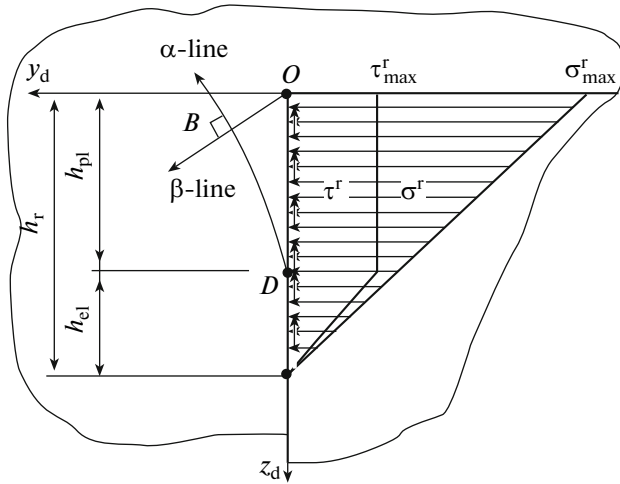


Fig. 2. Application of contact stress to the rear cutter surface.

The boundary α line passes through cutter tip O ($y_d = 0, z_d = 0$) perpendicular to the boundary β line and specifies the direction of the shear region

$$z_d = y_d + 2\mu_{r0}l_f \ln \left| \frac{l_f(1 - \mu_{r0})}{l_f(1 - \mu_{r0}) - y_d} \right|. \quad (10)$$

The point A of intersection of the boundary α and β slip lines is determined by numerical solution of the transcendental equation obtained by equating Eqs. (9) and (10).

Calculation of the plastic-zone boundaries show that the α and β lines are characterized by slight concavity, which increases with decrease in μ_{r0} . With increase in μ_{r0} , the inclination of the α lines to the y_d axis increases, while the inclination of the β lines decreases. With increase in μ_{r0} , the limiting plastic-friction coefficient at the front surface ($\mu_f = 0.5$) is attained fairly rapidly when beginning at the point $y_d = l_{pl}$. In that case, the external friction between the chip and the tool is zero, and the chip layer at the cutter is completely frozen. The formation of buildup or a stagnant zone begins; internal friction arises within the chip.

Plastic contact between the rear surface and cutting surface (Fig. 2) occurs at high slip rates. In physical terms, however, it is little different from the contact at the front surface. Consider the case when $\alpha_d = 0$ —in other words, with friction between the blank and the cutter's wear facet. The total contact length over the rear surface (h_r) is divided by point D into sections of plastic (h_{pl}) and elastic (h_{el}) contact.

To ensure uniform slip-line fields adjacent to the front and rear surfaces, the z_d and y_d axes are selected in opposite directions, with corresponding points of the α and β slip lines. The contact-stress distribution at the rear surface is assumed to be analogous to the stress distribution at the front surface. In other words, the normal stress σ_r corresponds to a triangle distribu-

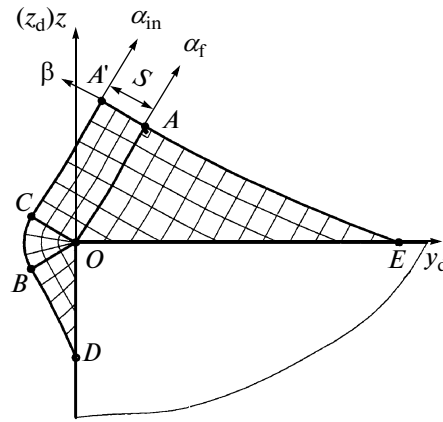


Fig. 3. Slip-line field in the secondary-deformation zone adjacent to the cutter.

tion, while the tangential stress τ_r is constant in the plastic section.

Then

$$\begin{cases} \tau^r = \tau_{\max}^r, & 0 \leq z_d \leq h_{pl}; \\ \tau^r = \frac{\tau_{\max}^r}{h_r - h_{pl}}(h_r - z_d), & h_{pl} \leq z_d \leq h_r; \end{cases}$$

$$\sigma^r = \sigma_{\max}^r \left(1 - \frac{z_d}{h_r} \right);$$

$$\mu_r = \mu_{r0} h_r / (h_r - z_d);$$

$$\mu_{r0} = \tau_{\max}^r / \sigma_{\max}^r.$$

If we know the variation of the frictional coefficient μ_r at the rear surface, then we may obtain the following expressions for the boundary lines, by proceeding as for the front surface

for the α lines

$$y_d = h_{pl} - z_d + 2\mu_{r0}h_r \ln \left| \frac{h_r(1 + \mu_{r0}) - h_{pl}}{h_r(1 + \mu_{r0}) - z_d} \right|; \quad (11)$$

for the β lines

$$y_d = z_d + 2\mu_{r0}h_r \ln \left| \frac{h_r(1 - \mu_{r0})}{h_r(1 - \mu_{r0}) - z_d} \right|. \quad (12)$$

By solving Eqs. (11) and (12), we determine the coordinates of the point B of intersection of the boundary slip lines.

The two slip-line fields adjacent to the front and rear surfaces may be connected through the centered fan COB (Fig. 3) and the region $OAA'C$ of almost uniform plastic deformation. The distance OC specifies the thickness s of the shear band of the cut layer between the initial α_{in} and final α_f slip lines. If $\mu_r = 0.5$ at point D , the blank will be completely frozen, and there is a possibility of buildup corresponding to region $EA' CBD$.

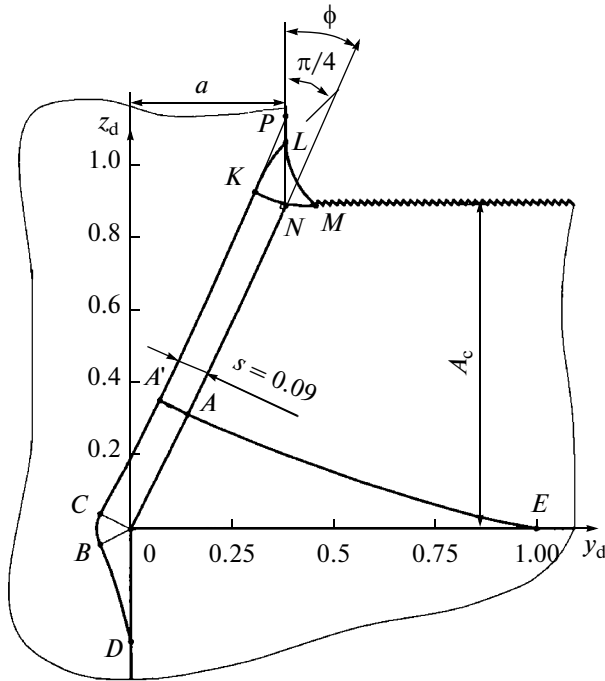


Fig. 4. Example of plastic-zone construction: $a = 0.4$ mm; $l_{pl} = 1$ mm; $h_{pl} = 0.3$ mm.

The position of the shear region of chip formation reaching the free surface of the cut layer and chip depends on the frictional conditions at the front and rear cutting surfaces. With no friction, the angle at which the slip planes reach the free surface would be $\pi/4$, as in the upsetting of a blank with lubricant during the pressure treatment of metals. These planes are known as Luders lines. The friction at the front surface is due to change in slip direction, which rotates counterclockwise. However, the condition of arrival at the free surface must be unchanged, since uniaxial compression by the primary normal stress occurs at point L (Fig. 4), while shear is inclined at $\pi/4$ to this direction [7]. Therefore, distortion of the slip direction must occur at the free surface. On that basis, the kinematically possible network of slip lines in the primary-deformation zone is plotted in Fig. 4. It is oriented relative to the previously plotted slip-line field in the cutter region so that the final boundary of the shear slip band is at the boundary α line OAN of the slip-line field at the front surface. The initial boundary $CA'K$ of the shear slip plane is equidistant from the final boundary OAN .

In region KLM adjacent to the angular transition between the external surfaces of the cut layer and the chip, the initial shear-band boundary rotates clockwise, thereby ensuring that it reaches the free surface at an angle $\pi/4$. The curves KL and KM will be segments of logarithmic spirals if we assume that the transition curve LM is part of a circle of radius R [2]. In this zone, the Cauchy problem of plasticity theory is solved [5]. To determine the characteristics of these spirals,

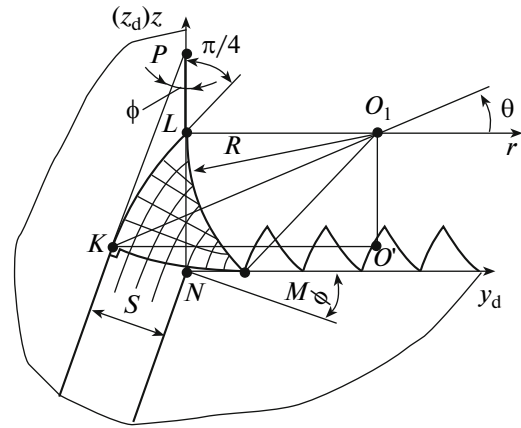


Fig. 5. Transitional plastic zone between cut layer and chip.

we consider triangle KLM separately (Fig. 5). In polar coordinates r, θ , centered at the point O_1 , the equation of the logarithmic spiral intersecting the whole radius vector at an angle $\pi/4$ takes the form [7]

$$r = ce^{\phi} \tag{13}$$

We may write the following condition for passage of the spiral in Eq. (13) through point L : $\theta_L = \pi$; $r_L = R$. Note that $\angle O_1KO' = \angle LO_1K = \pi/4 - \phi$, where ϕ is the shear angle (the shear-band inclination), which may be assumed to be the same for points P and N on account of the small curvature of the α slip line and the small size of zone KLM . Differentiating Eq. (10), we may express ϕ at point N as follows

$$\cot \phi = 1 + \frac{2\mu_{f0}l_f}{l_f(1 - \mu_{f0}) - a}$$

Then, for point K of the logarithmic spiral, $\theta_K = 5\pi/4 - \phi$; $r_K = O_1K = (R + s \cos \phi) / \cos(\pi/4 - \phi)$, where s is the shear-band thickness. Substituting the polar coordinates of points L and K into Eq. (13), we find that

$$\begin{cases} R = C_1 e^{\pi}; \\ \frac{R + s \cos \phi}{\cos(\pi/4 - \phi)} = C_1 e^{\frac{5\pi}{4} \phi} \end{cases}$$

Solving these equations, we obtain

$$\left. \begin{aligned} C_1 &= \frac{s \cos \phi}{e^{\pi} \left[e^{\frac{\pi}{4} - \phi} \cos\left(\frac{\pi}{4} - \phi\right) - 1 \right]} \\ R &= \frac{s \cos \phi}{e^{\frac{\pi}{4} - \phi} \cos\left(\frac{\pi}{4} - \phi\right) - 1} \end{aligned} \right\} \tag{14}$$

We may determine the position of the corners of the primary deformation zone in the coordinates y_d, z_d on

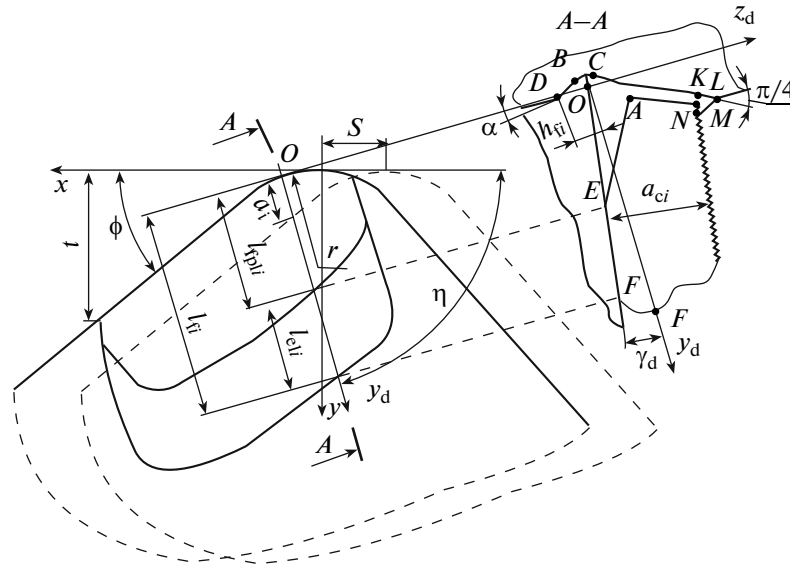


Fig. 6. Calculated stress–strain state in constrained cutting.

the basis of Eq. (14) and the finding that segment KM of the logarithmic spiral is symmetric relative to ray O_1K of segment KL (Fig. 4)

$$\begin{aligned} &L\{a; a_c + R\cos 2\phi\}; \\ &K\{a - s\cos\phi; a_c + s\sin\phi\}; \\ &M\{a + R(1 - \sin 2\phi); a_c\}. \end{aligned}$$

Note that, in the plastic triangle KLM , the free chip surface cannot intersect the boundary logarithm spiral KM at $\pi/4$, as our condition requires. We assume that point M is a bifurcation point, at which the saw-tooth external surface contour of the chip originates. Some of the saw teeth are parallel to curve LM ; others are segments of some internal α spiral of the given plastic zone (Fig. 5). In certain conditions specified by the properties of the blank and the stress–strain state, this saw-tooth structure is enlarged, with transition from continuous chip to fractured chip.

The thickness of the shear band s in Eq. (14) is determined as the distance from the coordinate origin to the intersection point B of the boundary α and β lines of the slip field adjacent to the rear surface (Fig. 4). As already noted, the coordinates of point B are found from Eqs. (11) and (12) by successive approximation. The calculations show that s increases with increase in contact length (wear) at the cutter’s rear surface.

Point N in Fig. 5 has the coordinates ($y_{d_N} = a$; $z_{d_N} = a_c$). Substitution in Eq. (10) yields

$$a_c = a + 2\mu_{r0}l_f \ln \left| \frac{l_f(1 - \mu_{r0})}{l_f(1 - \mu_{r0}) - a} \right|. \quad (15)$$

We now introduce the dimensionless parameter $m = l_f/a$, which characterizes the ratio between the

cut-layer thickness and the contact length of the chip and the front cutter surface. Given that $a_c = \zeta_a a$, we may write Eq. (15) in dimensionless form

$$\zeta_a = 1 + 2\mu_{r0}m \ln \left| \frac{m(1 - \mu_{r0})}{m(1 - \mu_{r0}) - 1} \right|. \quad (16)$$

Equation (16) is of fundamental importance, since it relates the chip-shrinkage coefficient, the frictional coefficient at the cutter tip, and the relative contact lengths. From any two of these parameters, the third may be determined.

These results apply to a plane stress–strain state. The calculation scheme for chip formation in constrained skew cutting by a blade with a rounded tip is shown in Fig. 6, together with one of the cross sections inclined at the chip departure angle. This cross section is constructed in the direction of chip departure at the front surface and coincides with the primary secant plane at the rear surface [1]. By successively considering a series of such cross sections, we may construct the three-dimensional plastic zone in constrained cutting. Here a_i is the cut-layer thickness in the chip departure direction for cross section i ; a_{ci} is the chip thickness for cross section i ; l_{fi} is the total contact length for cross section i ; l_{pli} is the plastic-contact length for cross section i ; l_{eli} is the elastic contact length for cross section i ; S is the supply; t is the cutting depth; r is the tip radius; ϕ is the primary plane angle; η is the chip departure angle; y_d is the reference axis of the dynamic coordinate system; γ_d is the front angle for cross section i in the dynamic coordinate system.

Thus, the slip-line field obtained for constrained cutting corresponds qualitatively to the shape of the plasticity zone established experimentally by means of microphotographs of continuous chip roots [2]. The field is also described analytically by specifying the key

coordinates and equations of the boundary slip lines. From these data, we may calculate the internal stress at any point of the plastic zone and hence the contact stresses at the cutter's working surfaces.

REFERENCES

1. Petrushin, S.I. and Proskokov, A.V., Theory of Constrained Cutting: Chip Formation with a Single Conditional Shear Surface, *Vestn. Mashinostr.*, 2009, no. 11, pp. 56–63.
2. Zorev, N.N., *Voprosy mekhaniki protsessa rezaniya metallov* (Mechanics of Metal Cutting), Moscow: Mashgiz, 1956.
3. Petrushin, S.I., *Vvedenie v teoriyu nesvobodnogo rezaniya materialov* (Introduction to the Theory of Constrained Cutting), Tomsk: Izd. TPU, 1999.
4. Armarego, E.J.A. and Brown, R.H., *The Machining of Metals*, Englewood Cliffs, New Jersey: Prentice Hall, 1969.
5. Goldschmidt, M.G., *Deformatsii i napryazheniya pri rezanii metallov* (Strain and Stress in Metal Cutting), Tomsk: STT, 2001.
6. Poletika, M.F., *Kontaktnye nagruzki na rezhushchikh poverkhnostyakh instrumenta* (Contact Loads at the Cutting Surfaces of Tools), Moscow: Mashinostroenie, 1969.
7. Storozhev, M.V. and Popov, E.A., *Teoriya obrabotki metallov davleniem* (Theory of the Pressure Treatment of Metals), Moscow: Mashinostroenie, 1977.